Proceedings of the ASME 32th International Conference on Ocean, Offshore and Arctic Engineering
OMAE2013
June 9-14, 2013, Nantes, France

OMAE2013-11200

NUMERICAL SIMULATIONS FOR INSTALLATION OF OFFSHORE WIND TURBINE MONOPILES USING FLOATING VESSELS

Lin Li, Zhen Gao, Torgeir Moan
Centre for Ships and Ocean Structures (CeSOS)
Norwegian University of Science and Technology(NTNU)
Otto Nielsens vei 10, NO-7491, Trondheim, Norway
Emails: lin.li@ntnu.no; zhen.gao@ntnu.no; torgeir.moan@ntnu.no

ABSTRACT

Monopiles are the most commonly used support structures for offshore wind turbines with up to 40m water depth due to the simplicity of the structure. The installation of turbine support structures can be carried out by a jack-up vessel which provides a stable working platform. However, the operational weather window using jack-up vessels is very limited due to the low sea states required for jacking up and down.

Compared to jack-up installation vessels, floating vessels have more flexibility due to fast transportations between foundations. However, the vessel motions will affect the motion responses of the lifting objects, which might bring installation difficulties. Therefore, it is necessary to examine the dynamic responses of the coupled system to ensure safe offshore operations.

In this paper, the installation operation of a monopile using a floating installation vessel is studied. Time domain simulations were carried out to study the installation process of a monopile, including lowering phase, landing phase and steady states after landing. Sensitivity studies were performed focusing on the effects by the gripper device stiffness and landing device stiffness. Comparisons of critical responses by using floating vessel and a jack-up vessel were also studied in the paper.

INTRODUCTION

Wind energy is proven to be one of the most promising renewable clean energy sources for future investment. As the available space with favorable wind conditions is getting scare onshore, offshore wind energy turns into an increasing attractive option due to the superior wind conditions associated with the vast offshore areas. However, offshore wind energy is facing great challenges. The main obstacle is the high costs in foundations, sea cables and of operation and maintenance work. Transportation and installation of offshore wind turbines is a critical phase of their life cycle. Compared with onshore work, offshore operations are much more risky and expensive, both from the financial and the engineering point of view. The unstable and choppy offshore environmental conditions are the first concern, which lead to more loads on the structure and cause severe risks. Due to the great environmental loads, larger support structures are called for, which will in turn raise challenge for offshore installations. Besides, the components of offshore wind turbines should be installed to very precise tolerances, so the weather window for the installation will be very limited [1]. Therefore, safety assessment of installation operations of offshore wind turbines in the design phase is of great importance.

Several different foundation structures for various water depths and soil conditions have been proposed for the offshore wind turbines (OWTs). For bottom-fixed OWTs, in general the industry prefers working with four types of foundations: gravity-based, monopile, jacket and tripod [2]. Among these, monopiles are the most commonly used foundations with up to 40m water depth due to the structural simplicity, less manufacturing and installation expenses. It is estimated that more than 75 % of all installations to date are founded on monopiles [3]. A typical monopile is a long tube with a diameter of 4 to 5 meters which is limited by the size of available driving equipment. It is driven into the sea bed by means of a very large hydraulic hammer if the soil condition is suitable. The constant pounding with the hammer in pile driven process leads to the steel becoming brittle and unsuitable for large load bearing. Therefore, the solution is to place a transition piece with a slightly different diameter on top of the monopile. The transition piece is pre-assembled onshore with a connecting flange for the tower, an access platform, ladders, tubes for

cables and other secondary structural members. The piece is connected with the monopile with an overlap length of around 1.5 times of the monopile diameter [4]. The annulus between the pile and the transition piece is grouted with high-density concrete and the transition piece is adjusted to true verticality. Figure 1 shows a typical offshore wind turbine substructure including a monopile and a transition piece.

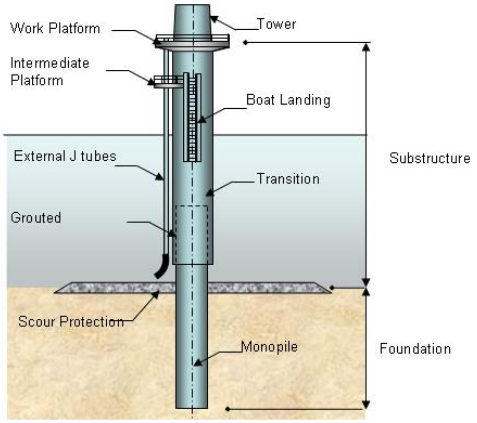

FIGURE 1. Monopile and transition piece for offshore wind turbines [5]

The installation of the monopile and the transition piece offshore are normally carried out by the same installation vessel. The installation process can be summarized into four main steps:

1) Upending the monopile from a horizontal position on the vessel to a vertical position. As the monopile is a very long structure, it is transported horizontally on the vessel and it should be upended to a vertical position with the aid of the onboard crane.

2) Lowering the monopile through the wave zone down to the sea bed. The hydrodynamic wave loads will induce the motions of monopile when it passes through the wave zone. The monopile should be landed to the designed point on the sea bed precisely.

3) Driving the monopile into the sea bed with a hydraulic hammer. The monopile is penetrating into the soil with the constant vertical pounding forces from the hammer.

4) Lifting the transition piece from the vessel and lowering it on top of the monopile. The transition piece is transported vertically on the vessel and it is lifted by the crane and lowered down on the top of the monopile.

The installation of turbine support structures can be carried out by a jack-up vessel [6][7][8] which provides a stable working platform for the lifting and piling operations. Jack-up vessels are also used for installation of wind turbine tower and rotor and nacelle assembly. However, the positioning operations of the jack-up vessel itself are time consuming and require very low sea states. The operational weather window using jack-up vessels will consequently be very limited which will increase the installation waiting time and thereby increase the costs. It is therefore interesting to investigate the feasibility of installing the support structures with floating installation vessels.

Compared to jack-up installation vessels, floating vessels [9][10] have more flexibility for offshore operations and will be effective in mass installations of a wind farm due to fast transportations between foundations. Hence, the potential of reducing installation costs by using floating installation vessel is huge. On the other hand, unlike the jack-up vessel which stands still on the sea bed, the motions of the floating installation vessel and the lifted objects are fully coupled during installation process and sensitive to the sea conditions. The vessel motions will affect the motion responses of the foundations, which might bring installation difficulties. Therefore, it is of importance to examine the dynamic responses of the coupled system during different phases of the installation in order to ensure safe offshore operations.

The purpose of this paper is to simulate the installation operation of a monopile using a floating installation vessel. In this study only step two in the installation process described above are taken into account. Upending and hammering of the monopile are not included.

Numerical simulations are carried out using the Marintek SIMO software [11][12]. A gripper device fixed on the vessel is simulated to control the horizontal motions of the monopile and to guide it lower towards the sea bed. When the pile lands on the seabed, a landing device is used in addition to guide the pile position to the designed point. All the simulations are performed in time domain considering stochastic wave conditions. Critical responses during each simulation case, such as motions of the lifted objects, contact forces between the monopile and the gripper or the landing devices and tensions in lifting wire are compared for different cases. Sensitivity studies were performed by considering important parameters for the operation, such as the stiffness of the gripper device and landing device. Comparisons of the responses with the same installation operations by using a jack-up vessel were also included.

SIMULATION MODEL

A floating installation vessel was chosen for the simulation. The main dimensions of the vessel can be found in Table 1. The vessel is a monohull heavy lift vessel. The crane is capable of performing lifts of up to 5000 tons at an outreach of 32 meters in fully revolving mode. The main hook features a clear height to the main deck of the vessel of maximum 100 meters. The vessel has been designed with a combination dynamic positioning (*DP*) system and eight-line mooring system. The positioning system allows for operations in shallow water and in very close proximity to other structures. Therefore, the lifting capacity and the positioning system of the floating vessel make it capable to perform the installation of monopiles in shallow water sites. The monopile used in the model was a long slender hollow cylinder with main dimensions listed in Table 1.

TABLE 1. Main parameters of the floating installation vessel and the monopile

Vessel		Monopile	
Length overall [*m*]	183.0	Total mass [*tons*]	500
Breadth [*m*]	47.0	Length [*m*]	60
Operational draught [*m*]	13.5	Outer diameter [*m*]	5.7
Displacement [*tons*]	52000	Thickness [*m*]	0.06

Figure 2 shows a schematic layout of the operation arrangement. In practice, there are three main bodies in the monopile lifting model - the floating installation vessel, hook and the monopile. In current model, the sling between the monopile and the hook is assumed very stiff. Hence, the hook and the monopile can be seen as rigidly connected and modeled as one body for simplicity. Therefore, in the numerical model, only two bodies are considered: the floating vessel and the monopile. The crane is assumed rigidly connected to the vessel. The global coordinate system is a right-handed coordinate system, shown in Figure 2, with the following orientation is used: X axis points towards the stern, Y – towards starboard, and Z – upwards. The origin is located at [mid-ship section, center line, still water line].

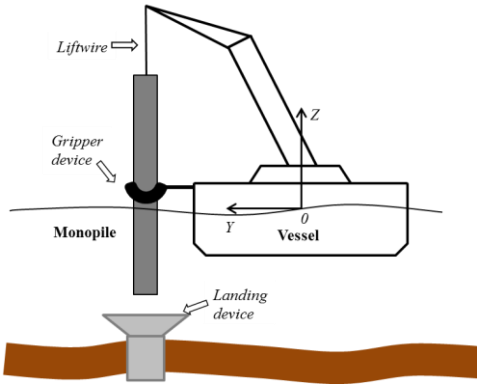

FIGURE 2. Lifting arrangement of the monopile

The motions of the crane tip will affect the responses of the whole lifting system. Thus, the crane tip position should be chosen carefully in practice. In present study, a representative coordinate of the crane tip in the global coordinate system of the model is: x = -40m, y = 30m, z = 73.5m.

There are two types of couplings between the vessel and the monopile: the wire coupling through the main lift wire and the coupling on the gripper device. A winch is connected to the crane tip and the lift wire can be extended through the winch so as to lower the monopile. The function of the gripper device is to control the horizontal motions of the monopile during lowering and landing. It will also support the monopile during driving operations. The gripper is also rigidly fixed on the vessel. The z-coordinate of the gripper is set as 4.5 meters above the still water and the horizontal coordinates equal to the mean values of the horizontal coordinates of the monopile axis at initial static position. A landing device in the seabed is included to guide the landing of the monopile to the designed point.

THEORETICAL BACKGROUND

The software SIMO has been used for dynamic analysis. SIMO is a non-linear time domain program for dynamic analysis of an operation system consisting of surface vessels and various other bodies. For the coupled system of a floating vessel and the monopile, there are 12 degrees of freedom (*DOFs*). The following twelve equations of motion are solved in a stepwise integration method [11].

$$\left(m+A(\infty)\right)\cdot\ddot{x}+D_1\dot{x}+D_2 f\left(\dot{x}\right)+Kx+\int_0^t h\left(t-\tau\right)\dot{x}\left(\tau\right)d\tau = q\left(t,x,\dot{x}\right) \quad (1)$$

m the total mass matrix of the vessel and the monopile;
A frequency-dependent added mass matrix;
D_1 linear damping matrix;
D_2 quadratic damping matrix;
K coupled hydrostatic stiffness matrix;
h the retardation function for the vessel, which is calculated from frequency dependent added mass or potential damping;
q external force vector, including wind force q_{WI}, 1st and 2nd order wave excitation forces $q^{(1)}{}_{WA}$ and $q^{(2)}{}_{WA}$, current force q_{CU} and any other forces q_{EXT}.

$$q\left(t,x,\dot{x}\right)=q_{WI}+q_{WA}^{(1)}+q_{WA}^{(2)}+q_{CU}+q_{EXT} \quad (2)$$

The coupled hydrostatic stiffness matrix K includes the hydrostatic stiffness of the ship, the stiffness from the mooring line, and the coupling between the vessel and the monopile via lift wire and gripper device.

The force model on the vessel and the monopile are described separately as follows.

Force model on the floating vessel

The potential added mass and damping coefficients, the hydrostatic stiffness as well as the first order wave excitation force transfer functions are all calculated in WAMIT based on panel method. Thus, the retardation functions in Eqn. (1) and the first order excitation force in Eqn. (2) can be obtained in SIMO using the input from WAMIT. Moreover, in the current vessel model, the following simplifications are applied for the vessel force model:

1) Waves are considered as main factor, and wind and current forces are not included;
2) Second order wave drift forces could induce slow-drift motions of the vessel mainly in surge, sway and yaw. It is assumed that the dynamic position system on the vessel is efficient enough to control the slow-drift motions. Hence, the second order wave drift forces are removed in the model. Therefore, the exciting forces for the floating vessel in the model only consists of the first order wave excitation force vector $q^{(1)}{}_{WA}$.
3) The mooring line systems are simplified by adding linear stiffness and damping terms in surge, sway and yaw.

For the mooring system simplification, the linear stiffness in surge, sway and yaw are calculated assuming the natural period in the three *DOFs* equal to 90 *sec*, which is a reasonable value for this type of vessel. Then, the stiffness could be obtained by Eqn. (3).

$$K_{ii} = \left(\frac{2\pi}{T_{i0}}\right)^2 \cdot \left(m_{ii} + A_{ii}\right), \quad i = 1,2,6 \tag{3}$$

where T_{i0} is the natural period for the i^{th} *DOF*, here T_{i0} = 90 *sec*, m_{ii} and A_{ii} are the mass and potential added mass respectively. The damping effects from the mooring system are non-linear, and the total damping must be determined by stochastic linearization. Here we use simplified linear damping to estimate the viscous damping from mooring system. According to the DNV-OS-E301[13], the damping coefficient in surge, sway and yaw in the model can be chosen as 10%, 20% and 15% of critical damping, respectively. Critical damping is given by Eqn. (4).

$$B_{ii} = 2\sqrt{K_{ii} \cdot \left(m_{ii} + A_{ii}\right)}, \quad i = 1,2,6 \tag{4}$$

where K_{ii} is the stiffness, and m_{ii} and A_{ii} are the mass and potential added mass, respectively.

Force model on the monopile

The external forces on the monopile include gravity force, buoyancy force, and hydrodynamic wave forces.

The diameter of the monopile is relatively small compared with the wave length. For a wave period from 5 *sec* to 12 *sec*, the wave length to the diameter ratio is from 7 to 30 for a water depth of 25 meters. For a wave height of 5 meters, the wave height to the structure diameter ratio is less than 1. In this case, the inertial force is the governing force. Furthermore, the motion of the monopile is large; thus, the linear theory from the panel method is not applicable. The instantaneous position of the monopile must be accounted for at each time step. Then, the Morison formula should be used. The monopile can be simulated as a slender body by using the strip theory. Therefore, the horizontal wave force $f_{W,s}$ per unit length on each strip of a vertical moving circular cylinder can be determined by Morison's equation[14].

$$\begin{aligned} f_{W,s} = {} & \rho_w C_M \frac{\pi D^2}{4} \cdot \ddot{\zeta}_s - \rho_w \left(C_M - 1\right) \frac{\pi D^2}{4} \cdot \ddot{x}_s \\ & + \frac{1}{2} \rho_w C_q D \cdot |\dot{\zeta}_s - \dot{x}_s| \cdot (\dot{\zeta}_s - \dot{x}_s) \end{aligned} \tag{5}$$

In the equation, positive force direction is the wave propagation direction. $\ddot{\zeta}_s$ and $\dot{\zeta}_s$ are water particle acceleration and velocity at the center of the strip; $\ddot{x}_s$ and $\dot{x}_s$ are the acceleration and velocity at the center of the strip due to the body motions; D is the outer diameter of the cylinder; C_M and C_q are the mass and quadratic drag force coefficients, respectively.

The first terms in the equation are wave excitation force, including diffraction and Froude-Krylov force (*FK* term). The second term is the inertial term and the third term is the quadratic drag term. C_M and C_q are dependent on many parameters like Reynolds number (*Re*), Kaulegan-Carpenter number (*KC*) and surface roughness ratio [14].

The outer surface of the monopile is assumed to be smooth, and *Re* number is in the magnitude of 10^6 to 10^7. The *KC* number in the operational sea states is in the range of 1 to 3. According to DNV-RP-C205 [15], the quadratic drag coefficient can be chosen as C_q = 0.7.

The monopile is a bottomless cylinder, and there is water with free surface inside the cylinder when it is submerged. This amount of water influences the hydrodynamic coefficients of the cylinder. Moreover, the submerged length of the cylinder increases with time. Therefore, it is necessary to investigate the hydrodynamic coefficients of the bottomless cylinder considering time varying submergence.

The added mass coefficients of the monopile with different submergences were calculated in HydroD (the solver is WAMIT) [16]. The results from HydroD were the 3D hydrodynamic added mass of the whole body. However, in order to use the strip theory to simulate the hydrodynamic forces in SIMO, 2D coefficients are required. Hence, the 2D added mass coefficients were obtained by dividing the 3D coefficients with submerged length. The water depth considered was 25 meters and the wave periods were from 5 *sec* to 12 *sec*.

The results showed that the 2D added mass coefficients increased with submerged length. However, for submergences larger than 5 meters, the 2D added mass coefficients approached to a constant of about 1.8 in the wave periods concerned. Furthermore, the total excitation forces were calculated by using Morison's equation and the strip theory with the 2D added mass coefficients as input, and were compared with 3D excitation forces calculated in HydroD. Very good agreements were obtained for submergence larger than 5 meters. As the responses for submergence less than 5 meters were less critical compared with larger submergences, an asymptotic value of 1.8 was chosen as the 2D added mass coefficient. Hence, in the numerical model the mass coefficient in the Morison's equation in Eqn. (5) was C_M = 2.8.

As observed, when the submerged length was large, the 2D added mass coefficient from the bottomless cylinder was about twice as the value from the cylinder with bottom. This means the water inside the cylinder behaves as 'frozen water'. Therefore, when modeling the monopile, each strip of the body can be divided into three components, which are illustrated in Figure 3.

1) Component 1 is the steel structure of the cylinder. It always contributes to the total mass of the body. When the strip is submerged, the displacement of water from component 1 is the only contribution to the buoyancy force.
2) Component 2 represents the added mass from water inside the cylinder. It contributes to the total mass of the body only in horizontal plane and it is counted for only when the strip is submerged.
3) Component 3 represents the added mass from the water outside the cylinder. It has the same properties as component 2.

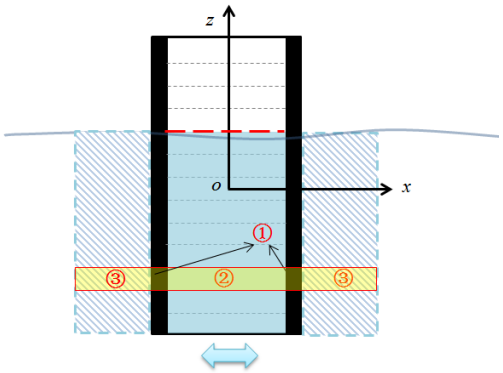

FIGURE 3. Modeling of forces for slender element using the strip theory

By defining the volume or mass of the three components above, all the matrix terms for each strip can be calculated. All the distributed forces are then integrated along the pile to obtain the total force and moment. It should be mentioned that as the wall thickness of the monopile is very small the hydrodynamic force in vertical direction was omitted. Besides, the effects of water exchanging and flow separation at the end of the monopile were not considered.

Wire coupling forces

The couplings between the vessel and the lifting bodies are realized by lift wires. The wire coupling force is modeled as a linear spring force according to [11]:

$$T = k \cdot \Delta l \qquad (6)$$

where T is the wire tension; Δl is the wire elongation and k is effective axial stiffness, which is given by:

$$\frac{1}{k} = \frac{l}{EA} + \frac{1}{k_0} \qquad (7)$$

where E is modulus of elasticity; A is the cross-section area of the wire, and k_0 is the crane flexibility. Knowing the position of the two ends of the wire, the elongation and thereby the tension can be determined. The material damping in the wire is included, and the damping per wire length is chosen as 2% of EA value [12].

The wire stiffness affects the natural frequencies of the whole lifting system, and influences the responses of the system significantly. Therefore, the wire properties should be carefully selected. In the numerical model, the properties of the wire coupling force term are shown in Table 2.

TABLE 2. Properties of the lift wire

Initial length [m]	EA [kN]	k_0 [$kN^{-1}m$]	Material damping [kNs]
6.0	2.0E+5	5.0E-5	4.0E+3

Docking cone coupling forces

Both the gripper device and the landing device (a template on the sea bed) are modeled in SIMO by 'docking cone coupling' [11]. The docking cone coupling is simulated as a guide pin attached on the lowering object and a docking cone fixed on the other body or on the sea bed. The funnel shaped cone has two parts: the conical part (opening diameter D_{c1}, height H_{c1}) and the cylindrical part (diameter D_{c2}, height H_{c2}), which are illustrated in Figure 4. The docking cone shape parameters used in present simulations are shown in Table 3. The conical part guides the pin to enter the cone and provides both axial and radial forces. After a success entering, the cylindrical part of the cone only provides forces in radial direction to keep the pin inside the cone.

TABLE 3. Docking cone shape parameters

D_{c1} [m]	H_{c1} [m]	D_{c2} [m]	H_{c2} [m]
2.0	3.0	0.1	5.0

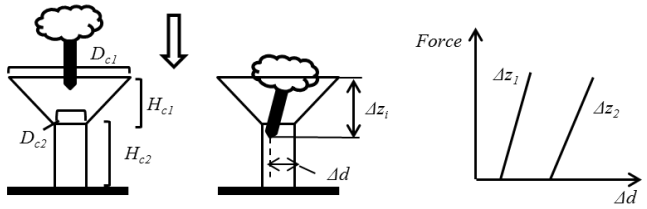

FIGURE 4. Illustration of docking cone coupling and force model

The contact forces are calculated based on the relative position of the guide pin and the cone. The stiffness of the docking cone can be defined by specifying the relative distance between the pin and the cone axis at different axial positions. Interpolation is applied for all the other axial positions. The force model is shown in Figure 4.

When using the docking cone coupling to model the gripper device, the cone is fixed to the monopile and the guide is fixed on the vessel. The cone is modeled only with a cylindrical part and only gives horizontal forces. Both the guide pin and the cone are moving with the attached bodies. For the landing device, the docking cone is fixed on the sea bed, while the guide pin is on the monopile. The docking cone for landing has both conical and cylindrical part to guide the monopile land on the designed position.

It should be noticed that for each pair of docking cone coupling the guide pin is defined as one point, which means it could not give any moments. This would result in large rotational motions of the body, i.e. the monopile can rotate around the tip where the guide pin of the landing device is attached. Therefore, for the gripper device, two pairs of couplings are applied with two guide pins at different vertical positions related on the vessels and thereby can provide moments to the pile. For the landing device, two pairs of docking cone and guide pin are modeled with opposite directions to provide both forces and moments. One cone is fixed at the sea bed with the guide pin on the monopile, and the other cone is attached on the monopile with the guide pin at the opening of the first cone.

TIME DOMAIN SIMULATIONS

Time domain simulation methods

Step-by-step integration methods were used to calculate the response by using an iterative routine. The third order Runge-Kutta-like method was used for numerical iteration [11]. The 1st order wave forces for the vessel were pre-generated by Fast Fourier Transformation (*FFT*) at the mean position. The wave particle motions for calculation of hydrodynamic forces on the monopile were calculated in time domain due to the time varying submergence of the pile.

The total dynamic simulation time for each case was 20 minutes. The winch started to run at 300 *sec* to avoid initial transient effects. The winch speed was 0.05 *m*/*sec*, and the winch stopped at 800 *sec*. Thus, the total lowering length was 25 meters. During the winch running time, the monopile lower tip went through splash zone and entered into the sea bed landing device. After the winch stopped, the dynamic simulation continued with the monopile and the vessel system in a steady state. During the whole process, the gripper device provided horizontal forces to the monopile.

In the time domain simulation, the time step must be carefully determined. The time step must be small enough to capture the highest frequency of the resonant phenomena. The natural periods of the monopile are shown in Table 4. The natural periods were calculated with monopile at three different positions by assuming the vessel was fixed. In the initial positions, the monopile was in air. Only gripper device provided horizontal stiffness and the wire length was the initial length. In the transition position, the pile was lowered 20 meters by the winch and the lower tip was just above the landing device. In the final position both landing device and gripper device contribute to horizontal stiffness. The wire length in the final position was 25 meters longer than in the initial position. The highest frequency in the system was the roll/pitch natural frequencies in the initial position. Furthermore, to capture one cycle of phenomena in the time domain, about 15 time steps are required. Therefore, the time step should be smaller than the roll/pitch natural period (0.73 sec) divided by 15. The time step in the simulation was finally chosen as 0.01 *sec*.

TABLE 4. Natural periods of the monopile (rigid-body motion, case: V2G2L2[refer to Table 5])

Motion	Initial position	Transition position	Final position
Surge [*s*]	1.19	2.0	1.56
Sway [*s*]	1.19	2.0	1.56
Heave [*s*]	1.33	1.86	2.01
Roll [*s*]	0.73	5.16	1.51
Pitch [*s*]	0.73	5.16	1.51
Yaw [*s*]	40.04	40.04	40.04

The environmental conditions for the time domain simulations in this study were selected as H_s=2.5*m*. The spectrum wave period (T_p) has been varied, from 5 *sec* to 12 *sec*, thus covering a realistic range. Only wave direction (*Dir*) of 45 degree was considered. For each combination of H_s and T_p, the irregular waves were modeled by the 6-parameter *JONSWAP* spectrum. For each case, simulations for different realizations of irregular waves were carried out to account for the variability of waves.

Convergence test

The lowering and landing processes of the monopile have transient effects by the nonlinear loads due to waves. In order to get reliable results, it is important to make sure a good convergence of the numerical model. By running 30 different realizations (random seed number) of each irregular wave case, the motions and responses from each seed can be compared with the mean values of all the 30 samples. Besides, an accumulative averaged value for seed number *i* (the mean value from seed 1 to *i*) can be calculated, indicating the speed of convergence.

The whole dynamic simulation can be divided into three main phases, which will be discussed in the next section. The convergence of dynamic responses from all the three phases was checked. The main responses concerned in the convergence study are the motions of the monopile tip, the lift wire tension, the contact forces from the gripper device and landing device. Figure 5 shows an example of the convergence in the landing phase from 30 random seeds. It can be seen from the figure that 30 seeds were enough to obtain convergent results for the extreme responses concerned. In present study, 30 seeds were used for each case, and the mean values of the extreme responses from all the seeds are used for detailed analysis and comparisons between different cases.

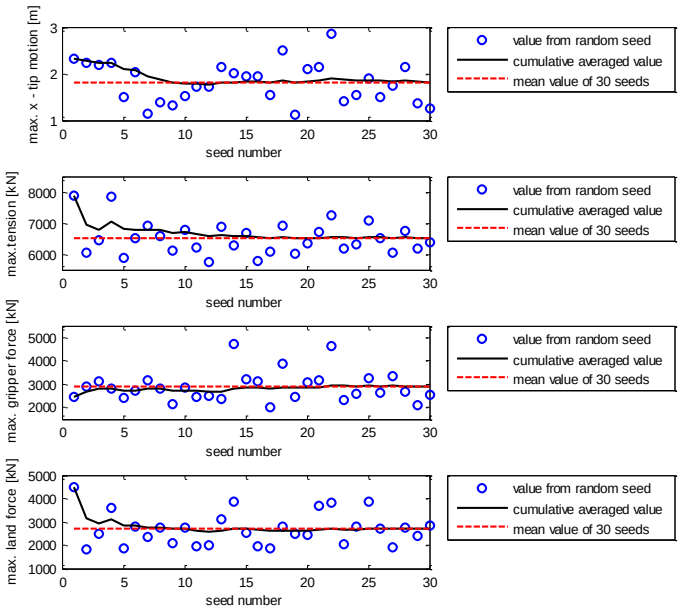

FIGURE 5. Convergence test results (Hs=2.5 m, Tp=6.0 s, Dir=45 deg, Case: V2G1L1, [refer to Table 5])

Sensitivity study

Sensitivity studies were performed in the numerical simulations. The studies compared the effects of the following parameters to the responses: installation vessel type, the gripper device stiffness and the landing device stiffness.

a) Installation vessel

Two types of vessels were considered in the simulations: a jack-up installation vessel and the floating installation vessel described in previous section. The purpose is to compare the performance of the two types of vessels to carry out the installation operation of a monopile.

The floating vessel was modeled as large floating body with 6 degrees of freedom. The motions of the vessel and the lifting objects are coupled together by lift wire and gripper device. The jack-up vessel was modeled as a bottom-fixed structure, and there were no motions transferring from the vessel to the lifting system.

b) Gripper device stiffness

The gripper device provides horizontal forces for the monopile in order to reduce the motions in waves during lowering. As described in previous section, the horizontal forces depend on the stiffness of the device and relative distance between the guide pin and the cone axis. Larger gripper stiffness will control the horizontal motions at the gripper position better compared with small stiffness. However, large contact forces will give huge impact on the gripper which might damage the structure. Therefore, it is necessary to study the effect of the stiffness of the gripper device to the monopile motions and contact forces. Two gripper stiffnesses were considered in the sensitivity study.

c) Landing device stiffness

Similar to the gripper device, two landing device stiffnesses were studied to evaluate the effects on the responses of the lifting system.

The parameters considered in the sensitivity studies are summarized in Table 5. For simplicity, abbreviations are used to represent the corresponding values.

TABLE 5. Sensitivity study parameters

Parameter	Value 1	Abbre-viation 1	Value 2	Abbre-viation 2
Vessel type	Jack-up	*V1*	Floating vessel	*V2*
Gripper stiffness [*kN/m*]	4000	*G1*	8000	*G2*
Landing stiffness [*kN/m*]	4000	*L1*	8000	*L2*

RESULTS AND DISCUSSIONS

Response time series

Figure 6 shows an example of the time history of critical responses: the monopile end tip positions, the landing contact force and the lift wire tension. As shown, the whole lowering process of the monopile can be divided into three phases.

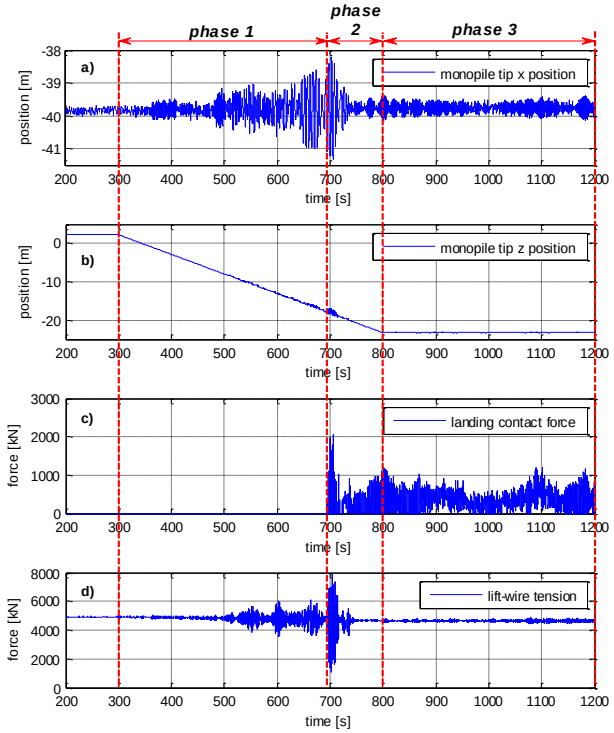

FIGURE 6. Time history of lowering and landing a monopile. (Hs =2.5 m, Tp=6.0 s, Dir=45 deg, Case: V2G1L1-seed 1[refer to Table 5])

Phase 1: lowering phase. The winch starts running at 300 *sec*. The monopile is lowered into water and the pile tip passes though the splash zone until to the position just above the landing device. In phase one, the lift wire length is increasing, which decreases the natural frequencies of the lifting system. The landing contact force is always zero. The *z*-position of the monopile is decreasing and the wave forces acting on the monopile induce large horizontal motions. The contact forces on the gripper device provide certain controls on the monopile horizontal motions. It can also be observed that in the lowering phase, the responses did not always increase with increasing pile submergence.

Phase 2: landing phase. Phase two begins when the landing docking cone force is larger than zero. The monopile starts entering into the cone. The contact force from the conical section of the cone gives vertical forces on the pile at the initial phase of landing. Hence, the monopile will move in positive z direction which increases the z-position of the body. If the vertical contact forces are very large, slack wire might occur. The monopile tip firstly enters the conical section and then the cylindrical section. Hence, the horizontal motions are reduced gradually as it goes deeper in the cone. The maximum motions and forces in landing phase always occurred when the monopile tip was in the conical section of the landing docking cone.

Phase 3: steady state phase. Phase three starts at 800 *sec*, when the winch stops. After a successful landing, the pile enters into the cylindrical part of the landing device. The horizontal

motions of the pile tip are constrained by the device. In this phase, the stiffness of the lifting system is stable with fixed winch. The whole system is in a steady state.

For sensitivity study, it is more reasonable to compare responses by using different parameters at the same phase due to the time-varying properties of the system.

Response spectrum analysis

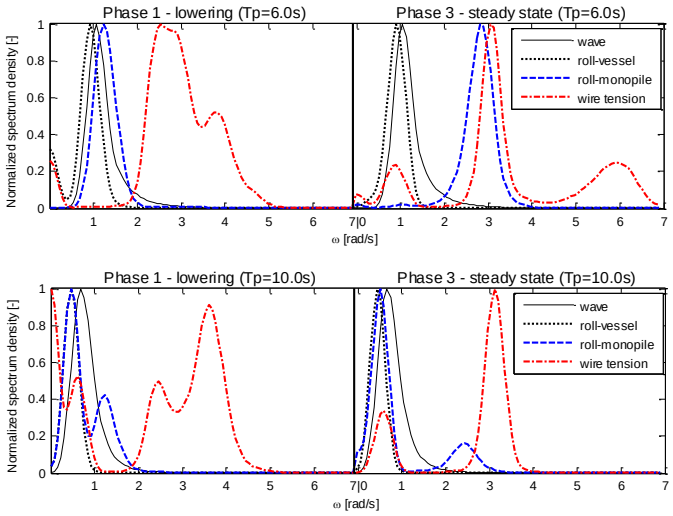

FIGURE 7. Normalized wave and response spectrums. (Hs =2.5m; Dir=45deg; Case: V2G2L2 [refer to Table 5])

TABLE 6. Normalization factors for spectrums in Figure 7

T_p	spectrum	Wave	Roll – vessel	Roll-monopile	Wire tension
[s]		$[m^2s/rad]$	$[deg^2s/rad]$	$[deg^2s/rad]$	$[kN^2s/rad]$
6.0	Phase 1	0.608	3.72E-3	0.889	4.32E+4
	Phase 3	0.608	3.93E-3	0.156	1.11E+3
10.	Phase 1	0.594	0.656	0.965	1.26E+4
	Phase 3	0.594	0.778	0.294	1.94E+4

The response spectrums for the lowering and steady state phases can be obtained from the time series. As the landing phase was very short and transient due to the contact of the monopile tip with the landing device, the spectrum in this phase was not studied.

Figure 7 shows two examples of response spectrums with Tp=6.0s and 10.0s, respectively. The wave spectrums are also shown in the figure. The responses considered here are the roll motions of the vessel and the monopile, as well as the lift wire tension. The spectrum density curves on the figures are the mean spectrum from 30 seeds and normalized by the maximum values, which are given in Table 6.

In short waves, the monopile roll motions were excited close to the main wave frequency range. The hydrodynamic wave loads on the monopile dominated the motions of the pile. As shown in table 4, the monopile rotational motion natural frequencies at transition position are close to the peak periods of short waves. Hence, the resonance effects in short waves during lowering were critical. The tension in phase one was dominated by the rotational motions of the pile, and the peak frequency was twice as large as roll spectral peak frequency. The heave motion also affected the tension during lowering. In steady state, the peak frequency of the pile roll motion corresponded to the roll natural frequency in the final position, and the tension was dominated by monopile heave motion.

In long waves, there were two peaks in the monopile roll motion spectrum in both phases. The secondary peak frequencies were the natural frequencies of the pile roll motion, while the main peak frequencies corresponded to the spectral peak frequencies of the vessel roll motion. This means in long waves, the monopile motions were dominated by the vessel motion. The wire tensions were dominated by the heave motion in long waves. The rotational motions of the monopile also affected the tension in lowering phase, while in steady state the effects from the vessel motion can be observed

Vessel type effects

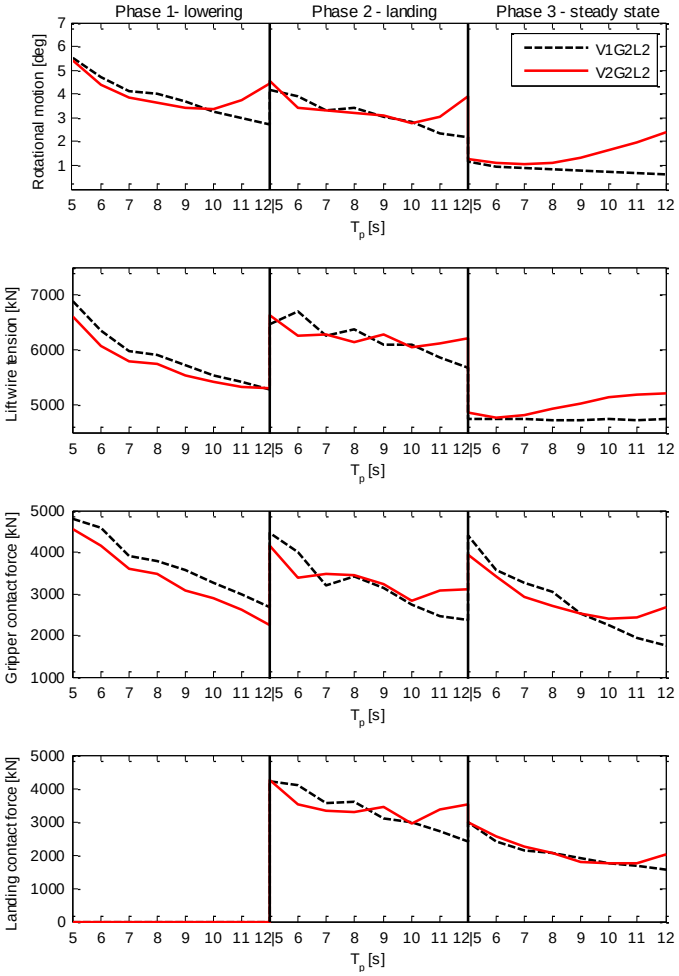

FIGURE 8. Responses by using different vessels (Hs =2.5 m, Dir=45 deg)

1) Responses by using jack-up vessel

Figure 8 shows the maximum values of critical responses during the three phases by using floating and jack-up vessels. The simulation cases in the figures are represented by abbreviations, and the definition of the abbreviations can refer to Table 5. The pile rotational motions in the figure are the maximum rotations of the pile referring to the horizontal plane and calculated by combining the pith and roll motions. It can be observed from the figure the responses of the lifting system were sensitive to the vessel type.

When jack-up vessel was used, the maximum forces and motions decreased with increasing wave spectral peak periods for all phases. The natural frequencies of the monopile rotational motions during lowering were close to the short wave peak periods (see Table 5 and Figure 7). The motions would be excited significantly in the short wave frequency range. In longer waves, the responses were smaller as the natural frequencies of the monopile were away from the main wave frequency range.

2) Responses by using floating vessel

The rotational motions of the monopile in the first two phases and the contact forces during landing were firstly decreased from short to intermediate waves and then increased in longer waves when the floating vessel was applied. This was mainly due to the influences from the crane tip motions on the floating vessel. Figure 9 shows one example of the maximum motions of the crane tip during lowering phase. It can be seen that the crane tip motions increased with increasing wave periods. In shorter waves, the crane tip motions were small and the effects on the monopile motions were limited. The motions of the monopile lifting system were dominated by the wave loads on the monopile and sensitive to shorter waves. As the wave periods increased, the crane tip motion increased significantly and dominated the motions of the monopile. Therefore, the rotational motions of the monopil and the contact forces during landing increased in longer waves.

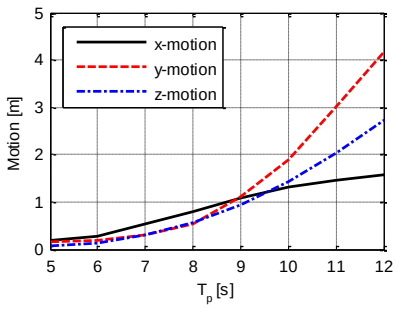

FIGURE 9. Maximum crane tip motions during lowering phase (Hs =2.5 m, Dir=45 deg, Case: V2G2L2 [refer to Table 5])

3) Comparisons of responses using different vessels

In the lowering phase, the lift wire tension and gripper device contact force using a jack-up vessel were larger than responses by using floating vessel. The crane tip motion on the floating vessel could compensate the relative motions between the crane tip and the lift point on top of the monopile, while for jack-up vessel the crane tip was fixed. However, as the crane tip motion increased greatly in long waves, the compensation effects would be minor compared in shorter waves. Similarly, the motions of the floating vessel would compensate the relative motions of the gripper device and the monopile, which reduced the gripper contact forces.

In landing phase, the responses by using a jack-up vessel were slightly larger in short waves, while in longer waves the responses by using the floating vessel were more critical. The reason was due to the effects from the increasing of crane tip motions in long waves.

In steady state phase, the rotational motions of the pile and the wire tension were larger when using the floating vessel, especially in long waves. In this phase, the monopile was controlled together by lift wire at the top, gripper device in the middle and landing device in the lower end. The crane tip horizontal motions could cause larger wire tension and induce larger rotational motions of the monopile when using the floating vessel. Moreover, the pile section in the gripper moved together with the vessel while the pile end tip was controlled by the landing device fixed on the sea bed, which would also induce larger rotational motions of the pile compared with the case using a jack-up vessel.

4) Comparisons of responses at different phases

In shorter waves, the monopile motion, lift wire tension and gripper contact force in the first two phases were both critical. In longer waves, largest responses happened at the landing phase due to the transient effects when the monopile started entering into the landing device. The responses in steady state were less critical when the wave periods were small, but they increased significantly in longer waves.

Gripper device stiffness effects

The effects by using different gripper stiffnesses on the responses of the lifting system are shown in Figure 10. In the figure the relative motions at the gripper device are the horizontal motions between the gripper device and the monopile.

As shown, the monopile rotational motion and the lift wire tension in lowering and landing phases were reduced somewhat when the gripper device stiffness increased. In the steady state phase, the effects of the gripper device stiffness on the pile motion and wire tension were minor.

However, the gripper contact force and the relative motions between the pile and the gripper device were very sensitive to the gripper stiffness. The gripper contact forces in lowering and landing phases were significantly increased when using higher stiffness. In steady state phase, the effects of the gripper stiffness on the contact force were less compared with the first two phases. The relative motions at the gripper device were reduced greatly with larger gripper stiffness.

In practice, the gripper device is a rigid structure and its connection with the vessel is flexible. Hence the stiffness of the gripper in this paper refers to the stiffness of the connection device. The relative motion between the monopile and the gripper device refers to the deformation of the connection device, which should be limited in a certain level. Therefore, the stiffness of the connection should be chosen properly in order to control the deformation of the structure and ensure the operability.

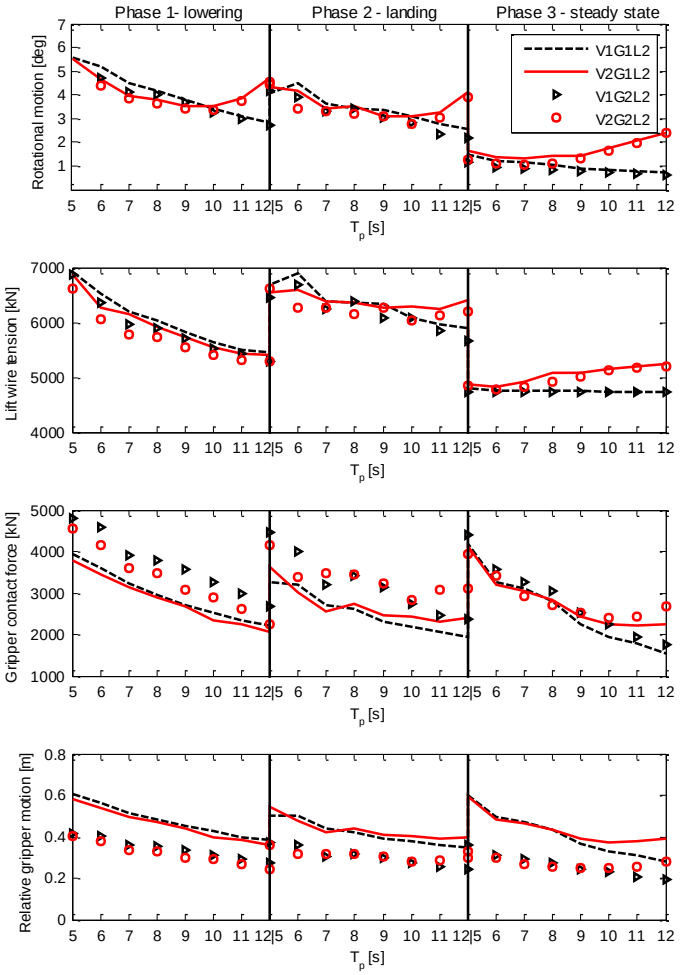

FIGURE 10. Responses by using different gripper stiffnesses and vessels (Hs =2.5m, Dir=45deg)

Landing device stiffness effects

Figure 11 presents the maximum responses by using two different landing device stiffnesses *L1* and *L2*. The monopile tip motions in the figure are the extreme offsets of the pile end tip from the axis of the landing device.

As shown, the landing stiffness had no effects on the lowering phase, and the monopile rotational motion and the lift wire tension were not sensitive to landing device stiffness.

However, the landing contact forces were greatly affected by the landing stiffness. In the landing phase, the maximum landing contact forces using stiffness *L2* were about 1.4 times as large as using stiffness *L1*. The maximum monopile tip motions were slightly reduced in this phase.

In the final phase, the landing contact forces were increased when larger stiffness was applied. The motions of the pile tip decreased greatly with increasing stiffness. From marine operation point of view, enough landing stiffness is necessary to control the pile tip motions in the landing device in order to accelerate the pile penetrating into the soil.

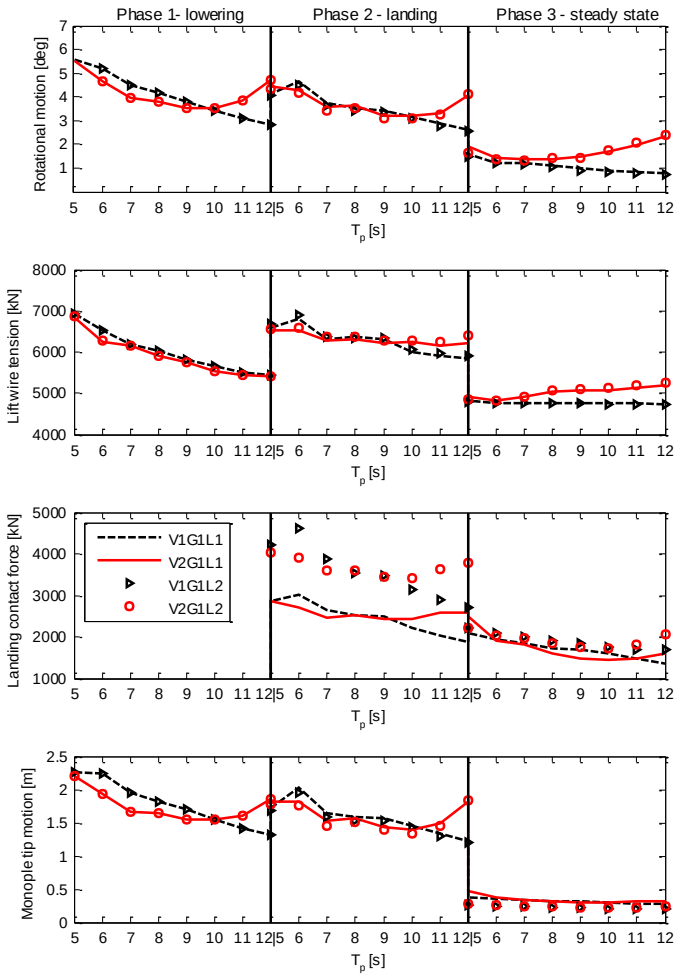

FIGURE 11. Responses by using different landing stiffnessses and vessels (Hs =2.5m, Dir=45deg)

CONCLUSIONS

Numerical models for installation of an offshore wind turbine monopile were established in SIMO with the focus on the phase of lowering the pile from above the sea water to the sea bed. The model included a floating installation vessel and a monopile. The couplings between the vessel and the monopile were realized by lift wire and gripper device. A landing device was also modeled to guide the lowering of the monopile into sea bed. Several assumptions and simplifications were made in

the force modeling both for the floating vessel and the monopile.

Time domain simulations were carried out for H_s = 2.5 *m*, T_p = 5*sec* to 12*sec* and *Dir* =45*deg*. Due to the transient effects in the process, 30 random realizations for irregular waves are needed to obtain good convergences for critical responses concerned.

The whole process can be divided into 3 phases: lowering, landing and steady states phases. The properties of the numerical model were changing from phase to phase. The responses from different phases were analyzed separately. This paper also compared the responses of the lifting system by using different vessel type, gripper device stiffness and landing device stiffness. The following conclusions are drawn from this study:

1) The monopile rotational motions are excited by wave loads on the pile in short waves, while in longer waves the motions are mainly induced by the floating vessel motions.

2) When a jack-up vessel is used, the lifting system is more sensitive to shorter waves. The responses reduce with increasing T_p. However, the responses were reduced from short to intermediate waves and increase in longer waves when using the floating vessel.

3) The vessel type affects the rotational motions of the monopile. The rotations by using a floating vessel are much larger than using a jack up vessel in long waves due to the influence of the vessel motions.

4) Gripper device stiffness affects the gripper contact forces and the relative motion of the monpile and gripper device significantly. Proper gripper device stiffness should be selected to control the relative motion.

5) The landing contact force in the landing phase increases greatly by using larger landing stiffness. Larger landing stiffness also provides better control on the pile end tip motion in steady state, which could be beneficial for the pile penetrating into the soil by its self-weight.

The limitations of the current numerical model and possible future work are discussed as follows:

1) The stiffness of gripper and landing devices in the model were assumed values. In practice, these properties should be derived from the real structures.

2) The contact forces acting on the monopile, the gripper and landing device are huge. Structural analysis under the contact forces may be necessary to ensure a safe operation.

3) The wire stiffness would influence the responses of the system by changing the natural frequencies of the system. Moreover, the crane tip coordinate dominates the crane tip and gripper device motions. Sensitivity study on the wire stiffness and crane tip position could also be interesting.

4) The sea states in present study only focused on H_s = 2.5 *m* and wave direction *Dir* =45*deg*. More sea states with different wave directions could be included to compare the performance of the system by using jack-up and floating vessels.

5) The 2nd force was not included in the floating vessel force model. If the floating vessel has slowly drift motions, the effects on the lifting system will be increasing.

6) The diffracted waves due to the presence of the floating vessel and the radiated waves induced by the motions of the vessel could influence the wave field of the monopile. Moreover, the hydrodynamic coefficients of the monopile might be increased when it is close to the vessel. These effects should be investigated in the future work.

REFERENCES

[1] Twidell, J. and Gaudiosi, G. (2008) Offshore Wind Power. Multi-Science Publishing Co. Ltd

[2] Kurt E. T. (2012) Offshore wind - A comprehensive guide to successful offshore wind farm installation. Academic Press

[3] Moeller, A. (2008) Efficient offshore wind turbine foundations. POWER EXPO 2008:International Exhibition on Efficient and Sustainable Energy.

[4] WindEnergie, G. L. (2004). "Guidelines for the Certification of Offshore Wind Turbines." Final Draft, Edition.

[5] Wind Energy – The Facts (WindFacts). European Wind Energy Association (EWEA). URL: http://www.wind-energy-the-facts.org/ (Date of access: 29.10.2012)

[6] Kim, Y. K., Shin, J. R. and Yoon, D. Y. (2012). A Design of Windmill Turbine Installation Vessel Using Jack-Up system. Proceedings of the 22nd International Offshore and Polar Engineering Conference, Rhodes, Greece

[7] Jack-up installation vessels. URL: http://www.a2sea.com/fleet/installation_vessels.aspx (Date of access: 29.10. 2012)

[8] Service Jack. URL: http://www.master-marine.no (Date of access: 29.10.2012)

[9] Oleg Strashnov - 5000-mt crane vessel. URL: http://www.seawayheavylifting.com.cy/ (Date of access: 29.10.2012)

[10] Heavy Lift Vessel Svanen. URL: http://www.offshore-energy.nl/page_9945.asp (Date of access: 29.10.2012)

[11] SIMO (2010). SIMO Theory Manual, Version 3.6, MARINTEK. Trondheim, Norway.

[12] SIMO (2010). SIMO User's Manual, Version 3.6, MARINTEK. Trondheim, Norway.

[13] DNV (2010). DNV OS E-301 Offshore Standard: Position mooring.

[14] Faltinsen O. M.(1990), Sea Loads on Ships and Offshore Structures, Cambridge University Press

[15] DNV (2010). DNV RP C-205 Recommended Practice: Environmental conditions and environmental loads.

[16] DNV (2011). SESAM User Manual-HydroD, Version 4.5.